Cardiovasc Intervent Radiol (2009) 32:62–69
DOI 10.1007/s00270-008-9462-x

CLINICAL INVESTIGATION

Radiofrequency Ablation Assisted by Real-Time Virtual Sonography and CT for Hepatocellular Carcinoma Undetectable by Conventional Sonography

Motoki Nakai · Morio Sato · Shinya Sahara · Isao Takasaka · Nobuyuki Kawai · Hiroki Minamiguchi · Hirohiko Tanihata · Masashi Kimura · Nozomu Takeuchi

Received: 16 January 2008 / Accepted: 8 October 2008 / Published online: 6 November 2008
© Springer Science+Business Media, LLC 2008

Abstract Real-time virtual sonography (RVS) is a diagnostic imaging support system, which provides the same cross-sectional multiplanar reconstruction images as ultrasound images on the same monitor screen in real time. The purpose of this study was to evaluate radiofrequency ablation (RFA) assisted by RVS and CT for hepatocellular carcinoma (HCC) undetectable with conventional sonography. Subjects were 20 patients with 20 HCC nodules not detected by conventional sonography but detectable by CT or MRI. All patients had hepatitis C-induced liver cirrhosis; there were 13 males and 7 females aged 55–81 years (mean, 69.3 years). RFA was performed in the CT room, and the tumor was punctured with the assistance of RVS. CT was performed immediately after puncture, and ablation was performed after confirming that the needle had been inserted into the tumor precisely. The mean number of punctures and success rates of the first puncture were evaluated. Treatment effects were evaluated with dynamic CT every 3 months after RFA. RFA was technically feasible and local tumor control was achieved in all patients. The mean number of punctures was 1.1, and the success rate of the first puncture was 90.0%. This method enabled safe ablation without complications. The mean follow-up period was 13.5 month (range, 9–18 months). No local recurrence was observed at the follow-up points. In conclusion, RFA assisted by RVS and CT is a safe and efficacious method of treatment for HCC undetectable by conventional sonography.

Keywords Radiofrequency ablation · Real-time virtual sonography · Hepatocellular carcinoma · CT hepatic arteriography · CT during arterial portography · MRI

Introduction

Percutaneous ethanol injection and radiofrequency ablation (RFA) have been widely performed as a method of local treatment for hepatocellular carcinoma (HCC) [1–4]. We have generally used B-mode sonography (conventional sonography) to detect and display HCC for percutaneous ethanol injection and RFA treatment. When the tumor is located below the diaphragm or deep within the liver, the target lesion for RFA is often obscure on conventional sonography. In addition, smaller lesions such as well-differentiated HCCs cannot be detected clearly on conventional sonography, and determination of residual viable portions of HCC after transcatheter arterial chemoembolization (TACE) and RFA is often difficult on conventional sonography.

Recent advances in CT and MRI have enabled the synthesis of high-quality multiplanar reconstruction (MPR) images. Real-time virtual sonography (RVS; Hitachi Medical, Tokyo) is a diagnostic imaging support system which can synchronize with B-mode ultrasound images. RVS provides the same cross-sectional MPR images as ultrasound images on the same monitor screen

M. Nakai (✉) · M. Sato · S. Sahara · I. Takasaka · N. Kawai · H. Minamiguchi · H. Tanihata · M. Kimura
Department of Radiology, Wakayama Medical University, 811-1 Kimiidera, Wakayama-shi, Wakayama 641-8510, Japan
e-mail: momonga@wakayama-med.ac.jp

N. Takeuchi
Department of Radiology, Hidaka General Hospital, 116-2, Sono, Gobo-shi, Wakayama 644-8655, Japan

in real time, using DICOM (Digital Imaging and Communication in Medicine) volume data from CT or MRI [5, 6]. The position of the sonographic probe is detected using a magnetic sensor, high-speed processing of DICOM volume data is performed using the sonographic apparatus, and MPR images on the same section as ultrasound images can be displayed in real time. The effectiveness of RVS has been reported by Hirooka et al. [5], and it was reported that RVS-guided RFA treatment could achieve better treatment efficacy for HCC [7–10]. We also expect that RFA assisted by RVS and CT can improve treatment efficacy for HCC which is not identified by B-mode sonography.

In the present study, we evaluated the safety and usefulness of RFA assisted by RVS and CT for HCC undetectable by conventional sonography.

Subjects and Methods

Patients

From August 2005 to September 2006, 20 patients with 20 HCC nodules, consisting of 13 males and 7 females aged 55–81 years (mean, 69.3 years), were enrolled in this study (Table 1). These nodules could not be visualized on conventional sonography but were detected by intravenous contrast-enhanced CT or MRI. All patients had hepatitis C-induced liver cirrhosis (Child-Pugh A, 14; Child-Pugh B, 6) and high levels of tumor markers (α-fetoprotein [AFP] or protein induced by vitamin K absence II [PIVKA-II]). HCC was diagnosed using imaging analysis, including dynamic CT or MRI with an intravenous bolus injection of contrast material, angiography, CT hepatic arteriography

Table 1 Patient data

No.	Gender	Age	Tumor location	Tumor size (mm)	Child-Pugh classification	AFP (ng/ml)/ PIVKA-II (mAU/ml)	Characteristics	RVS reference image	Needle	No. of punctures	Follow-up (mo)	Local recurrence
1	F	56	S8	29	A	69/21	Post TACE	CT	Cool-tip	1	18	(–)
2	M	65	S7	25	A	44/34.1	Without TACE	CT	Leveen	1	18	(–)
3	M	75	S8	24	A	30.4/159	Post TACE	CT	Cool-tip	1	18	(–)
4	M	72	S8	27	B	242.3/26	R-HCC	MRI	Leveen	1	18	(–)
5	M	70	S7	22	A	74.2/38	Post TACE	CT	Leveen	2	15	(–)
6	M	77	S7	20	B	30.1/14	R-HCC	MRI	Leveen	1	15	(–)
7	F	74	S8	28	A	161.4/81	Post TACE	CT	Leveen	1	15	(–)
8	M	74	S7	25	A	15.6/222	Post TACE	CT	Leveen	1	15	(–)
9	F	78	S8	25	A	10.4/120	Post TACE	CT	Leveen	1	15	(–)
10	M	65	S4	26	A	229.3/92	Post TACE	CT	Cool-tip	1	15	(–)
11	F	78	S5	22	B	41.0/196	Post TACE	CT	Leveen	1	12	(–)
12	F	74	S8	32	A	74.9/40.1	Without TACE	Modified CTHA	Leveen	1	12	(–)
13	M	62	S8	23	A	140.7/43.7	R-HCC	MRI	Leveen	2	12	(–)
14	M	63	S8	27	B	17.2/60	R-HCC	MRI	Leveen	1	12	(–)
15	F	56	S7	18	B	14.5/61	Without TACE	Modified CTHA	Leveen	1	12	(–)
16	F	81	S4	20	A	25.0/83	Post TACE	Modified CTHA	Leveen	1	12	(–)
17	M	70	S4	28	A	40.9/56	Post TACE	CT	Leveen	1	9	(–)
18	M	55	S7	23	B	94/22	Post TACE	CT	Leveen	1	9	(–)
19	M	71	S8	18	A	21.3/46	Without TACE	Modified CTHA	Leveen	1	9	(–)
20	M	69	S7	22	A	28.8/64	Without TACE	Modified CTHA	Leveen	1	9	(–)

Note: AFP, α-fetoprotein; PIVKA-II, protein induced by vitamin K absence II; TACE, transcatheter arterial chemoembolization; R-HCC, recurrent hepatocellular carcinoma previously treated with TACE; CTHA, CT hepatic arteriography

(CTHA), and CT during arterial portography (CTAP). Nine lesions were located in segment 8, seven in segment 7, three in segment 4, and one in segment 5. The maximum diameter of the HCC nodules ranged from 18 to 32 mm (mean ± SD, 24.2 ± 3.7 mm). Among the 20 patients, 11 had received TACE within 1 week before RFA in this series. Five patients were treated without prior TACE. Four nodules were recurrent nodules that developed after previous TACE. The nature of this study was fully explained to the patients, and informed consent was obtained from each of them. This study was performed with approval from our institutional ethics committee.

We performed TACE by selective introduction of a microcatheter into the segmental branch of the hepatic artery and injection of a mixture of anticancer drugs (mitomycin and farmorbicin; Kyowa Hakko, Tokyo) and iodized oil (Lipiodol; Bayer Schering Pharma, Osaka, Japan) followed by small particles of gelatin sponge.

Real-Time Virtual Sonography

The ultrasound device used included an RVS system (EUB–6500; Hitachi). The RVS system consists of a transmitter and magnetic sensor which detect the position of the sonographic probe. The transmitter was fixed to the CT stage, and a magnetic sensor was applied to the sonographic probe (Fig. 1). RVS provides the same cross-sectional MPR images as ultrasound images on the same monitor screen in real time, using DICOM volume data. Prior to RFA treatment, DICOM volume data from CT or MRI were loaded on the RVS apparatus. We synchronized B-mode ultrasound images with MPR images at the best timing of the inspiration.

Dynamic contrast-enhanced CT and CTHA were performed by 32 multidetector CT scanner (Aquilion 32, Toshiba Medical Systems Co, Ltd, Tokyo, Japan), and images reconstructed with a thickness of 1 mm were used for RVS. Dynamic contrast-enhanced CT consists of the arterial phase (35-s delay), hepatic portal phase (60-s delay), and hepatic venous phase (180-s delay), with intravenous bolus injection of nonionic contrast material (100 ml of 300 mg I/dl; Iopamiron; Bayer Schering Pharma, Osaka, Japan) at 3 ml/s. Hepatic venous images reconstructed with a thickness of 1 mm were used for 11 patients.

Modified CTHA was used for five patients and was performed for simultaneous depiction of HCC and intrahepatic vessels, using two catheters, with dual injection of contrast material. Nonionic contrast material (Iopamidol, 140 mg I; Daiichi-Sankyo, Tokyo) was injected via the superior mesenteric artery (SMA) and proper hepatic artery (PHA). Sixty milliliters of contrast material was injected at a rate of 3 ml/s via a 4-F catheter placed in the SMA, and

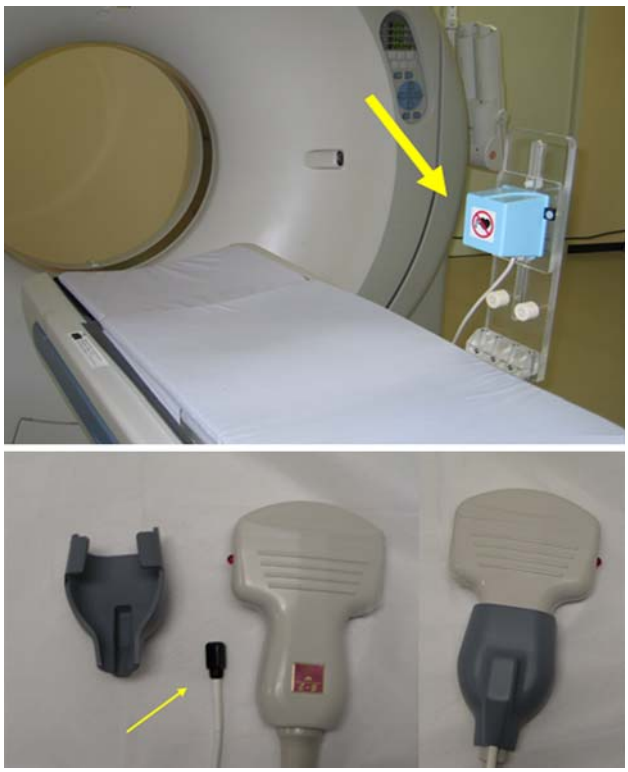

Fig. 1 Real-time virtual sonography at the time of RFA treatment. The transmitter was fixed to the CT stage (*thick arrow*), and a magnetic sensor was applied to the sonographic probe (*narrow arrow*)

30 ml of contrast material was injected at 2 ml/s via a 4-F catheter placed in the PHA 20 s after injection via the SMA (Fig. 2A). Modified CTHA was performed 30 s after the start of the first injection via the SMA. CT conditions for modified CTHA were as follows: helical pitch, 21; slice thickness, 1 mm; and scanning time, ~5 s. Prior to contrast material injection, 0.1 μg/kg of a vasodilative agent, PGEI (Taisho-Toyama, Tokyo), was injected into the SMA. All injections of contrast material were performed with a power injector (Dual Shot GX; Nemotokyorindo, Tokyo).

Dynamic gadolinium (Gd)-enhanced MRI was performed with three-dimensional spoiled gradient-echo T1-weighted MRI (three-dimensional volumetric interpolated breath-hold examination [3D-VIBE]; Siemens Germany; TR, 3.36 ms; TE, 1.38 ms; imaging time, 18 s; FOV, 360 × 270; matrix, 256 × 154; flip angle, 20°; band width, 490; fat sat, on) using a 1.5-T apparatus (Avanto, Siemens, Germany). Dynamic Gd-enhanced MRI consists of the arterial phase (25-s delay), hepatic portal phase (50-s delay), and hepatic venous phase (180-s delay), with intravenous injection of contrast material (20 ml of Magnevist [meglumine gadopentetate]; Bayer **Schering Pharma, Osaka, Japan**) at 3 ml/s. Arterial phase images reconstructed with a thickness of 3 mm were used for four patients with recurrent nodules.

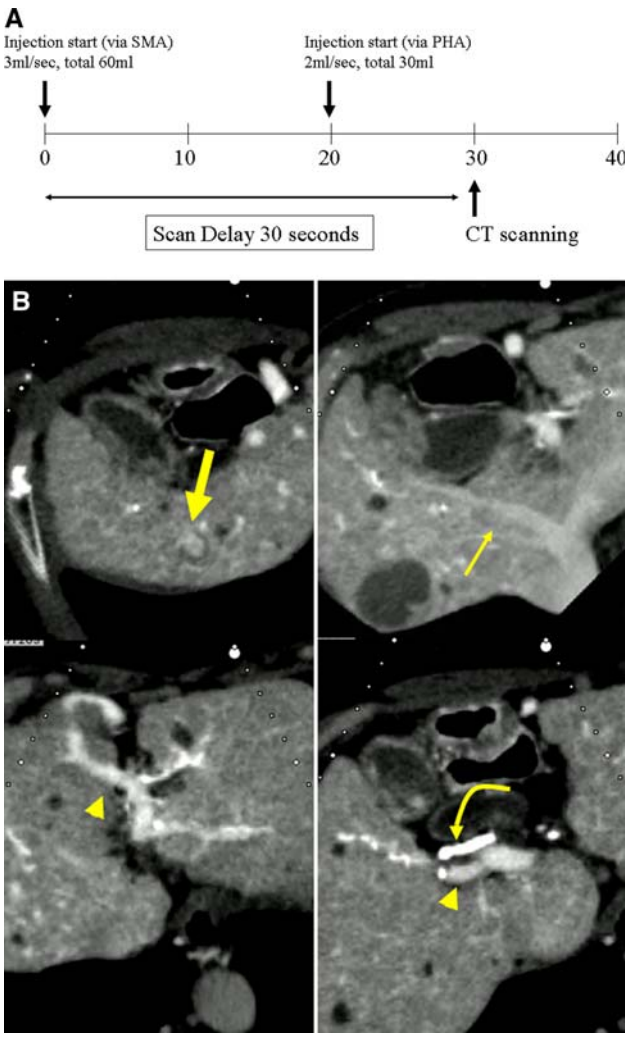

Fig. 2 **A** Injection protocol for modified CTHA for simultaneous depiction of the HCC, hepatic arteries, portal veins, and hepatic veins. Sixty milliliters of contrast medium was injected at a rate of 3 ml/s via the SMA, and then 30 ml of contrast medium was injected at 2 ml/s via the PHA 20 s later. Scan delay was 30 s. **B** A 56-year-old female patient with an HCC in the S7. MPR image using modified CTHA. The liver vasculature and HCC(*thick arrow*) were demonstrated simultaneously. Hepatic artery, curved arrow; portal vein, arrowhead; hepatic vein, narrow arrow

RFA Procedure

RFA was performed in the CT room. Before treatment, 15 mg of pentazocine and 25 mg of hydroxyzine hydrochloride were administered intramuscularly. Local anesthesia was induced by injection of 10 ml of 1% lidocaine through the skin into the peritoneum. RFA needles used were the Leveen needle (Boston Scientific, Natick, MA, USA) for 17 patients and the Cool-tip needle (Valleylab, Boulder, CO, USA) for 3.

Blood pressure, respiration, pulse, and electrocardiograms were continuously monitored. A ground pad was affixed to the thighs of the patients. Tissue impedance and power output status was monitored throughout the procedure. Ablation was completed when roll-off (or breakdown) occurred a second time.

RFA Assisted by RVS and CT

Prior to puncture, the three-dimensional (3D) anatomical relationships between the tumor and the diaphragm or intrahepatic vessels were sufficiently examined and the distances were measured on RVS. The tumor site surmised was punctured with the assistance of RVS, and CT was then performed immediately. CT images after puncture were reconstructed with a thickness of 1 mm at intervals of 0.5 mm and transferred to a 3D workstation (AZE, Virtual Place), where 3D images (maximum-intensity projection image and MPR image) were constructed. Needle insertion was confirmed with CT and 3D images immediately after puncture. After confirmation of needle insertion into the target tumor, ablation was performed. If the needle was not inserted into the tumor, the needle was pulled and removed and the tumor was punctured with RVS assistance again. The range of ablation was evaluated by two radiologists 1 week later with contrast-enhanced CT. If the necrotic area depicted on posttreatment dynamic CT was larger than the viable lesion on pretreatment CT, the treatment was considered successful. We evaluated the mean number of punctures and rates of success of the first puncture and RFA procedures. Follow-up dynamic CT scans were performed every 3 months after RFA and treatment effects were evaluated.

Results

The RFA needle was successfully inserted and RFA was successfully performed in all patients. The target HCC nodule and viable portion of the HCC could be detected with RVS in all patients. With modified CTHA, HCC, hepatic arteries, portal veins, and hepatic veins can all be depicted simultaneously (Fig. 2B). Ablation was safely performed in all patients after confirming with CT that the RFA needle had been inserted into the tumor (Figs. 3 and 4). After RFA, mild pain and fever were noted, but no severe complications occurred. Even the tumor lesions directly beneath the diaphragm were ablated without side effects such as injury of the diaphragm. No thermal injuries to adjacent structures or organs occurred. The puncture procedure was performed at most twice. The mean number of punctures was 1.1, and the rate of success of the first puncture was 90.0% (Table 2). Contrast-enhanced CT 1 week after RFA showed complete local tumor ablation in all patients. The mean follow-up period was 13.5 months

Fig. 3 A 65-year-old male patient with an HCC in the S7 hepatic dome. RFA was performed with a 3.0-cm Leveen needle. **A** Selective CTHA; **B** RVS image using enhanced CT; **C** CT after puncture; **D** MPR image after puncture; **E** contrast-enhanced CT 1 week after RFA; **F** Contrast-enhanced CT 6 months after RFA. The tumor was demonstrated in the S7 hepatic dome on selective CTHA via the right hepatic artery. The tumor was not visualized on sonography but was clearly detected with RVS imaging (*arrow*: tumor lesion). CT and MPR images after puncture demonstrated that the Leveen needle had been inserted into the tumor. Contrast-enhanced CT 1 week after RFA revealed a low-density area, indicating complete necrosis of the tumor. No local recurrence was noted on contrast-enhanced CT 6 months after RFA

(range, 9–18 months). No local recurrence was observed in any patients. RFA was technically feasible and local tumor control was achieved in all patients.

Discussion

The sonographic guidance method is most suitable for detecting and treating liver nodules and, therefore, has been performed most widely in percutaneous interventional treatment for HCC [11, 12]. However, nodules below the diaphragm and in deep from the body surface cannot be detected clearly on conventional sonography. With progression of cirrhosis, echo signals in the liver become heterogeneous, and identification of the target HCC nodule becomes difficult on conventional sonography. It has also been difficult to determine the residual viable portion of HCC after treatments such as TACE and RFA, because of the similarity in appearance of necrosis and viable tumor tissue on conventional sonography.

For HCC nodules undetectable by sonography, use of puncture methods under CT guidance [13, 14] and with intrathoracic injection of artificial pleural effusion [15, 16] has been reported. However, with puncture under CT guidance, puncture of the HCC nodule must be performed blindly and CT must be performed several times during the procedure. It was reported that pneumothorax was sometimes observed after CT-guided puncture [14]. In ultrasonically guided puncture with artificial pleural effusion, after a 5% glucose sterile solution (500–1500 ml) was

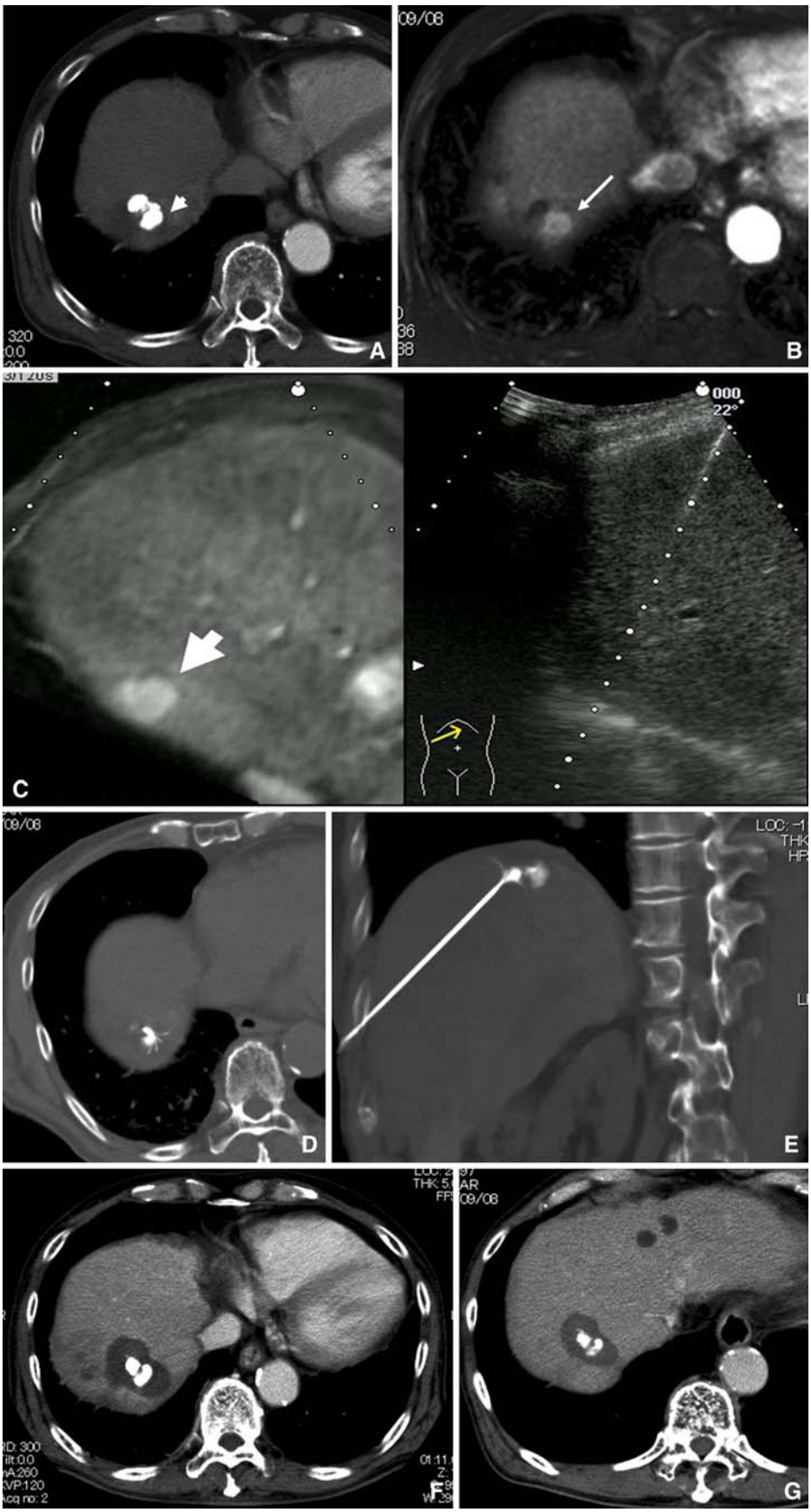

Fig. 4 A 77-year-old male patient with a recurrent HCC after previous TACE in the S7 hepatic dome. RFA was performed with a 2.0-cm Leveen needle. **A** Arterial-phase image on dynamic CT; **B** arterial-phase image of dynamic MRI; **C** RVS image using the arterial phase of dynamic MRI; **D** CT after puncture; **E** MPR image after puncture; **F** contrast-enhanced CT 1 week after RFA; **G** contrast-enhanced CT 12 months after RFA. Lipiodol had accumulated in the tumor (*arrowhead*), and determination of viable lesions and recurrence was difficult on dynamic CT because of Lipiodol deposition. Arterial enhancement was recognized in the left portion of the tumor on dynamic MRI (*narrow arrow*). The viable tumor lesion was not visualized on sonography but clearly detected on the RVS image (*wide arrow*). CT and MPR images after puncture demonstrated that the Leveen needle had been inserted into the tumor. Contrast-enhanced CT 1 week after RFA revealed a low-density area larger than the viable lesion. No local recurrence was noted on contrast-enhanced CT 12 months after RFA

Table 2 Mean number of punctures and rate of success of the first puncture and RFA procedures

Mean no. of punctures	1.1
Success of first puncture	90%
Success of RFA procedure	100%

injected into the pleural cavity to separate the lung and the liver, it became possible to obtain an image of the whole tumor. However, complications such as temporary mild cough and dyspnea and reduction of oxygen saturation of the blood have been reported [16]. In addition, some patients with adhesion of the pleura may not be indicated for artificial pleural effusion.

The target HCC nodule and viable portion of the HCC can usually be detected with contrast-enhanced CT or MRI. Therefore, even HCC nodules not visualized on conventional sonography are depicted clearly with RVS. It was reported that RVS-guided RFA treatment can achieve better treatment efficacy for HCC [7–10]. Hirooka et al. reported that the mean number of treatments with RVS was significantly lower than that without RVS [7]. Kitada et al. reported that the mean gap between the needle insertion line and the center of the tumor was 1.6 mm [9]. However, since RVS reference images provide virtual information, it is necessary to evaluate 3D anatomical relationships between the HCC nodules and the diaphragm or liver vasculature prior to puncture. Furthermore, needle insertion into the tumor should be confirmed on CT after puncture and before ablation. CT confirmation after puncture permits determination of whether or not the needle has touched the diaphragm or extended into the extrahepatic region and, thus, enables safe performance of RFA for HCC undetectable by conventional sonography without complications. Therefore, CT confirmation of needle insertion is important in this procedure. We used two kinds of needles, the Leveen needle and Cool-tip needle, in this study. The Leveen needle is a 17-gauge expansion-type electrode with a hook needle. The Cool-tip needle is a single 17-gauge electrode. While CT scanning after puncture, the former needle was fixed to the liver with hook without support. The hook needle was useful in this procedure assisted by CT.

In this study, we used CT and MRI data for RVS reference images. In arterial-phase images of dynamic studies, the HCC is depicted clearly, but liver vasculature such as the hepatic veins and portal veins is unclear. Minami et al. reported that the portal phase of CT images may be the most suitable to indicate the 3D relationship between the liver vasculature and tumors on RVS [10]. Tatsugami et al. reported an intravenous double-step injection of contrast material for the simultaneous depiction of HCC, portal veins, and hepatic veins in RVS [17]. CTHA and CTAP have been shown to have a high sensitivity for detecting hepatic tumors and to be capable of demonstrating subtle changes in the attenuation values of tumor nodules [18, 19]. In this study, we devised a modified method in which CTHA and CTAP were performed simultaneously. With modified CTHA, the HCC, hepatic arteries, portal veins, and hepatic veins were all depicted simultaneously, and evaluation of 3D anatomical relationships between HCC nodules and liver vasculature was easy. Modified CTHA was helpful in the simultaneous identification of HCC nodules and intrahepatic vessels under RVS and contributed to the accurate and safe performance of RFA for HCCs.

We used 3D-VIBE for MR scanning. 3D-VIBE can rapidly provide 3D images of the abdomen, which can be collected as isotropic voxel data suitable for maximum-intensity projection and MPR processing [20–22]. MRI images obtained by 3D-VIBE can be used for RVS due to their isotropic spatial resolution. Determination of the viability of lesions is usually evaluated with contrast effects on the arterial phase. Iodized oil (Lipiodol) is usually used in TACE. Determination of the viable portion or recurrence of the tumor after TACE is often difficult in contrast-enhanced CT because of Lipiodol deposition, though the contrast effects of the tumor can be evaluated by Gd-enhanced MRI regardless of Lipiodol deposition [23]. MRI is thus useful for RFA for viable lesions and recurrences after TACE. Furthermore, MRI can be performed without exposure to irradiation. However, at least 15 s of breath-holding is required for MRI scanning of the entire liver. Scanning time for MRI is much longer than for MDCT at present.

We have shown, with data including the rates of success of the first puncture and local recurrence, that RFA assisted by RVS and CT can be effective for treating HCC. Furthermore, no major complications were noted in any patients, indicating that our method of using assistance with RVS and CT is safe and efficacious for the treatment of HCC undetectable by conventional sonography.

References

1. Ebara M, Ohto M, Sugiura N, Kita K, Yoshikawa M, Okuda K, Kondo F, Kondo Y (1990) Percutaneous ethanol injection for the treatment of small hepatocellular carcinoma Study of 95 patients. J Gastroenterol Hepatol 5(6):616–626
2. Shiina S, Yasuda H, Muto H, Tagawa K, Unuma T, Ibukuro K, Inoue Y, Takanashi R (1987) Percutaneous ethanol injection in the treatment of liver neoplasms. AJR 149(5):949–952
3. Livraghi T, Goldberg SN, Lazzaroni S, Meloni F, Ierace T, Solbiati L, Gazelle GS (2000) Hepatocellular carcinoma: radiofrequency ablation of medium and large lesions. Radiology 214(3):761–768 [PMID: 10715043]

4. Rossi S, Di Stasi M, Buscarini E, Quaretti P, Garbagnati F, Squassante L, Paties CT, Silverman DE, Buscarini L (1996) Percutaneous RF interstitial thermal ablation in the treatment of hepatic cancer. AJR 167:759–768 [PMID: 8751696]
5. Hirooka M, Iuchi H, Kurose K, Kumagi T, Horiike N, Onji M (2005) Abdominal virtual ultrasonographic images reconstructed by multi-detector row helical computed tomography. Eur J Radiol 53(2):312–317
6. Tatsugami F et al (2007) Hepatic computed tomography for simultaneous depiction of hepatocellular carcinoma, intrahepatic portal veins, and hepatic veins in real-time virtual sonography: initial experience. J Ultrasound Med 26:1065–1069
7. Hirooka M, Iuchi H, Kumagi T, Shigematsu S, Hiraoka A, Uehara T, Kurose K, Horiike N, Onji M (2006) Virtual sonographic radiofrequency ablation of hepatocellular carcinoma visualized on CT but not on conventional sonography. AJR 186:S255–S260
8. Toshikuni N et al (2007) Virtual ultrasonography-assisted percutaneous ablation of hepatocellular carcinoma. Hepatogastroenterology 54(80):2361–2364
9. Kitada T et al (2008) Effectiveness of real-time virtual sonography-guided radiofrequency ablation treatment for patients with hepatocellular carcinomas. Hepatol Res 38:565–571
10. Minami Y et al (2007) Percutaneous radiofrequency ablation of sonographically unidentifiable liver tumors feasibility and usefulness of a novel guiding technique with an integrated system of computed tomography and sonographic images. Oncology 72(Suppl 1):111–116
11. Solmi L, Muratori R, Bertoni F, Gandolfi L (1993) Echo-guided percutaneous ethanol injection in small hepatocellular carcinoma: personal experience. Hepatogastroenterology 40(5):505–508
12. Seki T, Wakabayashi M, Nakagawa T, Itho T, Shiro T, Kunieda K, Sato M, Uchiyama S, Inoue K (1994) Ultrasonically guided percutaneous microwave coagulation therapy for small hepatocellular carcinoma. Cancer 74(3):817–825
13. Sato M, Watanabe Y, Tokui K, Kawachi K, Sugata S, Ikezoe J (2000) CT-guided treatment of ultrasonically invisible hepatocellular carcinoma. Am J Gastroenterol 95(8):2102–2106
14. Toyoda M, Kakizaki S, Horiuchi K, Katakai K, Sohara N, Sato K, Takagi H, Mori M, Nakajima T (2006) Computed tomography-guided transpulmonary radiofrequency ablation for hepatocellular carcinoma located in hepatic dome. World J Gastroenterol 12(4):608–611
15. Minami Y, Kudo M, Kawasaki T, Chung H, Ogawa C, Inoue T, Sakaguchi Y, Sakamoto H, Shiozaki H (2003) Percutaneous ultrasound-guided radiofrequency ablation with artificial pleural effusion for hepatocellular carcinoma in the hepatic dome. J Gastroenterol 38(11):1066–1070
16. Koda M, Ueki M, Maeda Y, Mimura K, Okamoto K, Matsunaga Y, Kawakami M, Hosho K, Murawaki Y (2004) Percutaneous sonographically guided radiofrequency ablation with artificial pleural effusion for hepatocellular carcinoma located under the diaphragm. AJR 183(3):583–588
17. Tatsugami F et al (2007) Hepatic computed tomography for simultaneous depiction of hepatocellular carcinoma, intrahepatic portal veins, and hepatic veins in real-time virtual sonography: initial experience. J Ultrasound Med 26(8):1065–1069
18. Murakami T, Oi H, Hori M, Kim T, Takahashi S, Tomoda K, Narumi Y, Nakamura H (1997) Helical CT during arterial portography and hepatic arteriography for detecting hypervascular hepatocellular carcinoma. AJR 169(1):131–135
19. Matsuo M, Kanematsu M, Inaba Y, Matsueda K, Yamagami T, Kondo H, Arai Y, Hoshi H (2001) Pre-operative detection of malignant hepatic tumours: value of combined helical CT during arterial portography and biphasic CT during hepatic arteriography. Clin Radiol 56(2):138–145
20. Rofsky NM, Lee VS, Laub G, Pollack MA, Krinsky GA, Thomasson D, Ambrosino MM, Weinreb JC (1999) Abdominal MR imaging with a volumetric interpolated breath-hold examination. Radiology 212(3):876–884
21. Lee VS, Lavelle MT, Rofsky NM, Laub G, Thomasson DM, Krinsky GA, Weinreb JC (2000) Hepatic MR imaging with a dynamic contrast-enhanced isotropic volumetric interpolated breath-hold examination: feasibility, reproducibility, and technical quality. Radiology 215(2):365–372
22. Kwak HS, Lee JM, Kim YK, Lee YH, Kim CS (2005) Detection of hepatocellular carcinoma: comparison of ferumoxides-enhanced and gadolinium-enhanced dynamic three-dimensional volume interpolated breath-hold MR imaging. Eur Radiol 15(1): 140–147
23. Murakami T, Nakamura H, Hori S et al (1993) Detection of viable tumor cells in hepatocellular carcinoma following transcatheter arterial chemoembolization with iodized oil Pathologic correlation with dynamic turbo-FLASH MR imaging with Gd-DTPA. Acta Radiol 34(4):399–403